REVIEW

National Science Review
2: 183–201, 2015
doi: 10.1093/nsr/nwv024
Advance access publication 11 May 2015

CHEMISTRY

Special Topic: Catalysis—Facing the Future

Understanding nano effects in catalysis

Fan Yang, Dehui Deng, Xiulian Pan, Qiang Fu and Xinhe Bao*

ABSTRACT

Catalysis, as a key and enabling technology, plays an increasingly important role in fields ranging from energy, environment and agriculture to health care. Rational design and synthesis of highly efficient catalysts has become the ultimate goal of catalysis research. Thanks to the rapid development of nanoscience and nanotechnology, and in particular a theoretical understanding of the tuning of electronic structure in nanoscale systems, this element of design is becoming possible via precise control of nanoparticles' composition, morphology, structure and electronic states. At the same time, it is important to develop tools for *in situ* characterization of nanocatalysts under realistic reaction conditions, and for monitoring the dynamics of catalysis with high spatial, temporal and energy resolution. In this review, we discuss confinement effects in nanocatalysis, a concept that our group has put forward and developed over several years. Taking the confined catalytic systems of carbon nanotubes, metal-confined nano-oxides and 2D layered nanocatalysts as examples, we summarize and analyze the fundamental concepts, the research methods and some of the key scientific issues involved in nanocatalysis. Moreover, we present a perspective on the challenges and opportunities in future research on nanocatalysis from the aspects of: (1) controlled synthesis of nanocatalysts and rational design of catalytically active centers; (2) *in situ* characterization of nanocatalysts and dynamics of catalytic processes; (3) computational chemistry with a complexity approximating that of experiments; and (4) scale-up and commercialization of nanocatalysts.

Keywords: nanocatalysis, confinement, carbon nanotubes, graphene, 2D materials, inverse catalysts, computational chemistry, *in situ* characterization

State Key Laboratory of Catalysis, iChEM (Collaborative Innovation Center of Chemistry for Energy Materials), Dalian Institute of Chemical Physics, Chinese Academy of Sciences, Dalian 116023, China

***Corresponding author.** E-mail: xhbao@dicp.ac.cn

Received 8 April 2015; **Revised** 13 April 2015; **Accepted** 13 April 2015

INTRODUCTION

Catalysis has been a core technology for many aspects of national economy, including petroleum refining, synthesis of fertilizers and other chemicals, and pollution control [1]. In recent years, the need for sustainable development of society has made stringent demands on the optimal utilization of natural resources. The chemical industry, which is closely related to energy generation, the environment, agriculture and health, is thus facing a major change, perhaps even a revolution. The development of the national economy in China also demands cleaner and more efficient utilization of fossil resources, such as the conversion of coal to natural gases, basic chemicals and liquid fuels, and the utilization of clean and renewable energy sources, including H_2–O_2 fuel cells, solar energy, biomass conversion and the conversion of carbon dioxide. Catalysis is the key enabling technology for confronting these challenges, and is itself undergoing major scientific and technological transformation and innovation. Our understanding of catalysis, which has been largely associated with the development of the petrochemical industry in the past century, will focus more on the activation and transformation of small molecules, with an emphasis on the control of catalysts and catalytic processes and the pursuit of 100% product selectivity under mild reaction conditions [2]. These changes depend on the development of new theories and methods in various aspects of catalytic research, such as catalyst preparation, theoretical simulation of catalytic processes, *in situ* characterization of catalysts and catalytic processes, and the scaling-up and industrialization of catalytic processes.

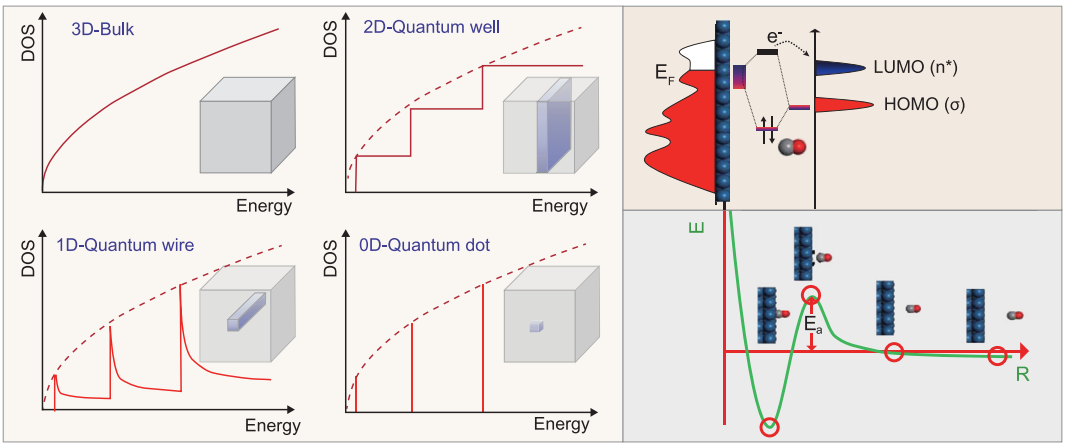

Figure 1. Schematic illustration of the modulation in DOS of various nanoscale systems (left), and electron transfer between an adsorbed molecule and a catalyst surface (right). LUMO: Lowest unoccupied molecular orbital; HOMO: Highest occupied molecular orbital.

Tailoring catalysts and catalytic processes have long been the 'Holy Grail' of catalytic chemistry—indeed, of much of chemistry as a whole. Research in catalysis over the past century has made it clear that key elementary steps of catalytic reactions, such as the adsorption of reactants, the diffusion of intermediates and the desorption of products, all involve electron transfer between the catalyst surface and the reactive species. Tuning of the spatial and energy distribution of valence electrons at the catalyst surface can thus be used to directly control catalytic properties such as the activation energy barrier, which determines the reactivity and the selection of reaction pathways, and thus product selectivity [3–9]. In principle, frontier molecular orbital theory can provide an understanding of key steps involved in surface catalytic reactions. The theory indicates that the strength of the adsorption and bonding of reactants on catalyst surfaces is closely related to the symmetry and spin state of reactant's molecular or atomic orbitals, and depends on matching the energy levels of the reactants to those of the catalyst surface as well.

For a long time, researchers tried to influence and adjust the surface structure and electronic state of a catalyst surface by mixing additives with the primary catalytic components, thus enhancing catalytic performance. Since the development of surface science from the middle of the last century, scientists have come to realize that even different faces of the same crystal could have a significantly different distribution of valence electrons due to their different atomic arrangements and interactions. This difference can lead to variations in molecular adsorption and reactivity on different crystal faces [10,11]. Norskov and coworkers invoked a so-called d-band center theory based on a large body of experimental and theoretical results, which emphasizes that the density of d-band valence electrons near the Fermi level is an important factor affecting catalytic reactions [12].

Meanwhile, the unique physical and chemical properties of nanoparticles (NPs) introduced with the development of nanoscience have attracted wide attention in a number of fields, including catalysis [13,14]. Valence electrons in bulk metals form continuous bands. When the bulk material is reduced in a certain direction down to the nanometer scale, the motion of electrons in this direction is subjected to confinement. Compared to bulk metals, NPs exhibit much larger total exposed surface areas and various combinations of surface structures, and electronic confinement effects within NPs may lead to major changes in the electronic structure (Fig. 1). This raises the possibility of tuning the catalytic process. In this sense, nanotechnology could provide an effective means through which we can effectively and quantitatively control the surface structure and electronic properties of supported nanocatalysts without changing their composition. It is thus hoped that adsorption and catalytic reactions can be optimized by continuously adjusting the size of catalysts at the nanometer scale.

Size effects in NPs have been noticed since the infancy of catalytic research, for example, through studies of ultrafine particles and single-site catalysts [15–19]. It has long been found that catalytic activities often increase with decreasing size of catalyst particles. However, it was traditionally thought that a decrease in particle size simply causes an increase in the proportion of surface species that are catalytically active, and also an increase in surface defects: these factors were generally considered to be primarily responsible for the size effect. But the development of nanoscience has led to an awareness that in addition to the increase in surface area

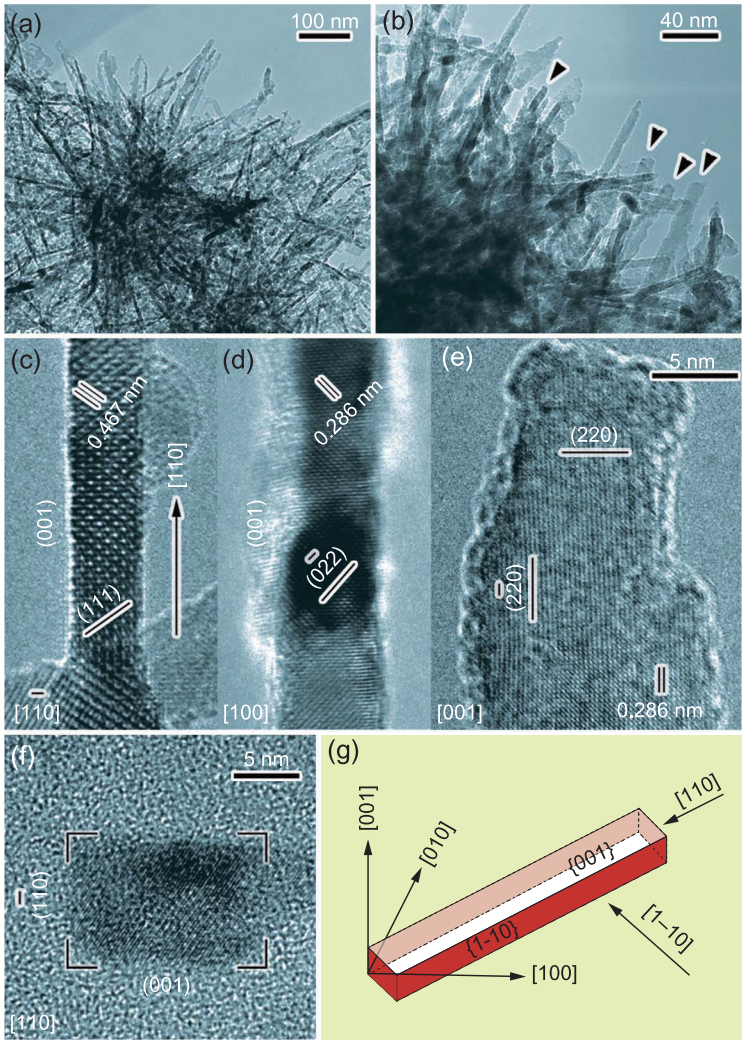

Figure 2. Typical TEM images of Co_3O_4 synthesized in the form of nanorods radiating from a cluster core in a coral-like morphology. These nanorods not only catalyze CO oxidation at temperatures as low as –77°C but also remain stable in a moist stream of normal feed gas. Adapted with permission from [23].

and heterogeneity of atomic structure, catalytic NPs exhibit quantum size effects in their electronic nature. Moreover, nanoscale pores also show unique electronic confinement effects [20–22]. Therefore, the marriage between nanoscience/nanotechnology and catalysis brings huge opportunities for the development of catalysis.

In recent years, there has been great progress in understanding nanoscale catalysts—for example, the effects of particle size and morphology, and the catalytic properties of 2D materials, nanophases of carbon and nanoporous materials. By tuning the morphology of catalysts at the nanoscale, one can quantitatively design and preferentially expose crystal faces that are highly active, thereby increasing the surface density of active sites (Fig. 2) [23]. Or one can reduce the size of catalytic NPs to a single atom or a 'pseudo-single' atom, thereby maximizing the catalytic activity of active components (Fig. 3) [24,25]. These studies have deepened our understanding both of nano effects in catalysis and of catalytic mechanisms in related processes. In the past two decades, our group has focused on the effect of confined electrons on the catalytic properties of nanosystems. We have systematically studied the correlation between the structures/electronic states and the catalytic properties of nanocatalytic systems, including nano-sized molecular sieves [26], nano-carbon materials [27] and nano-oxide materials [28,29], which are used in the conversion of carbon monoxide, syngas and methane. This review summarizes our experimental and theoretical results on how the nano effects play a role in tuning the electronic structure and subsequently the catalytic properties in such confined catalytic systems. We further elaborate on the concept of the 'confinement effect in nanocatalysis', which our group has put forward and developed.

CATALYSIS WITHIN CARBON NANOTUBES AND THE SYNERGETIC CONFINEMENT EFFECT

Carbon has been widely used as an adsorbent and catalytic material since synthetic forms of carbon were developed almost a century ago. Significant progress has been made over the years, both experimentally and theoretically, in controlled synthesis and in understanding the structures and catalytic properties of carbon materials including fullerenes, carbon nanotubes (CNTs), graphene, mesoporous carbon and activated carbon [30,31]. Catalysis by nanostructured carbon materials, especially CNTs, has received wide attention. Research groups, including those led by Centi, Schloegl, Serp and Su, have carried out extensive investigations on the acidity and basicity of oxygen-containing functional groups (e.g. hydroxyl, carboxyl and amino groups) at the edges and defect sites of nanostructured carbon, and their correlation with catalytic performance. For instance, Schloegl and coworkers demonstrated that the oxygen atoms on the defect sites of the outer surface of CNTs play a crucial role in the dehydrogenation of ethylbenzene [32].

CNTs can be envisioned as graphene layers rolling up to form a well-defined tubular structure. The π electron density of the graphene layers shifts from the concave inner surface to the convex outer surface because of the curvature, resulting in an electron potential difference across the CNT walls [33,34]. This endows CNTs with unique physico-chemical properties, distinct from other,

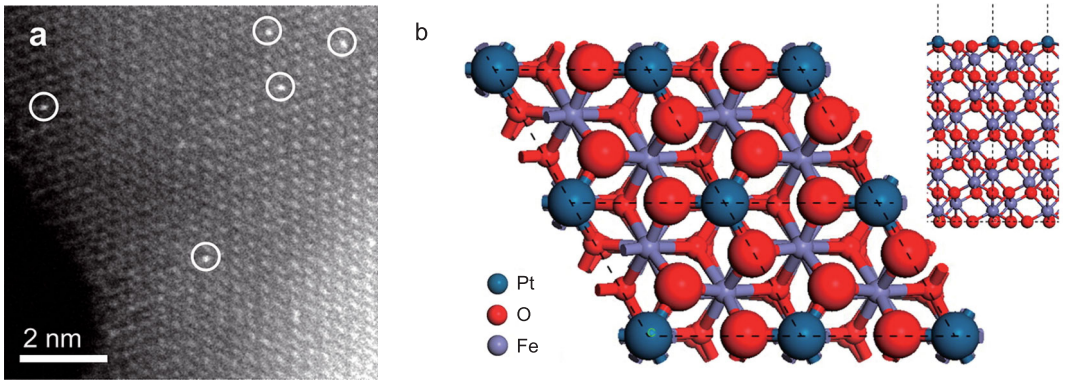

Figure 3. (a) High angle annular dark field scanning transmission electron microscopy (HAADF-STEM) image and (b) density functional modeling of Pt_1/FeO_x. Single metal atoms on support surfaces provide a unique opportunity to tune active sites and optimize the activity, selectivity, and stability of heterogeneous catalysts, offering the potential for applications in a variety of industrial chemical reactions. Adapted with permission from [25].

conventional carbon materials. Fig. 4 shows the electron potential difference between the concave and convex surfaces as a function of the CNT diameter, calculated from a simple model. A potential difference as high as 0.20 eV is estimated for a nanotube with a diameter of 1.36 nm, causing a strong electric field in the nanospace. Thus, if catalytic NPs are placed within such an environment, the nanospace not only exerts a physical restriction on them (and on the reactions they facilitate), but also provides a unique electronic microenvironment that modulates electron transfer processes [35–38].

A variety of methods have been reported to disperse NPs within the channels of CNTs [39–43]. We have developed an efficient approach for catalytic applications, which allows homogeneous dispersion of various metal NPs in CNTs with different diameters [44]. Briefly, the technique involves several steps (Fig. 5), including purification and cutting of long as-synthesized CNTs, followed by filling with NPs. In the first step, silver or iron NPs may be dispersed onto the outer walls of CNTs as oxidation catalysts, which could introduce defects on the surface of CNTs through controlled oxidation.

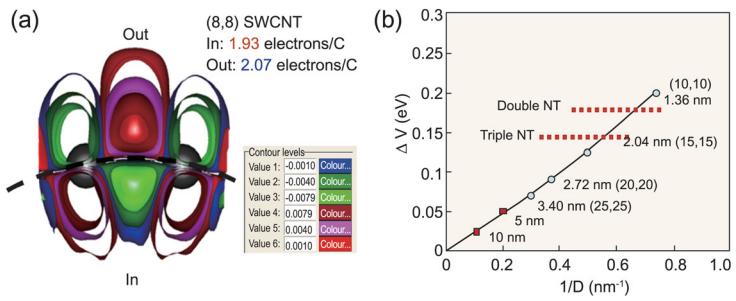

Figure 4. (a) The number of electrons on carbon atoms on the concave and convex surface of CNT (8,8). (b) Electron static potential difference inside and outside of CNTs as a function of tube diameter.

Long nanotubes are then shortened to the desired length (typically 100–500 nm) by cleaving them at these defects through etching with HNO_3. With ultrasound treatment, we are then able to introduce metal and metal oxide NPs efficiently into the CNT channels, usually with more than 75–85% of the particles located inside. The size of the NPs depends on the diameter of CNTs: for example, particles of 2–5 nm can be usually obtained within nanotubes with an inner diameter of 4–8 nm (Fig. 6 upper), while subnanometer-sized particles (<1 nm) are dispersed within the channels of single-walled CNTs (SWCNTs) and double-walled CNTs with inner diameters of 0.8–2 nm [45–47].

The capability of CNT channels to modulate the properties and behavior of confined molecules and nanomaterials is receiving increasing attention. Alterations in crystal structures, in chemical bonding and even in chemical state are frequently reported [48–51]. For example, we demonstrated the reduction of Fe_2O_3 NPs confined within CNTs: confinement in CNTs with an inner diameter of 4–8 nm leads to a reduction temperature 200°C lower than that required for Fe_2O_3 NPs on the outer walls of the same CNTs, as revealed by *in situ* transmission electron microscopy (TEM) and X-ray diffraction measurements [52]. Further studies showed that the reduction temperature lowers in a stepwise manner with decreasing inner diameter of CNTs (Fig. 6 below) [53]. Moreover, the oxidation of metallic Fe NPs is hindered by confinement: the apparent activation energy for oxidation is 4 kJ mol^{-1} higher than it is for the same NPs on the outside of the CNTs, suggesting that the oxidation rate (corrosion) can be retarded by confinement [53]. Density functional theory (DFT) calculations on Fe_9 clusters have provided insights into the underlying mechanism [54]. The d-band states of the

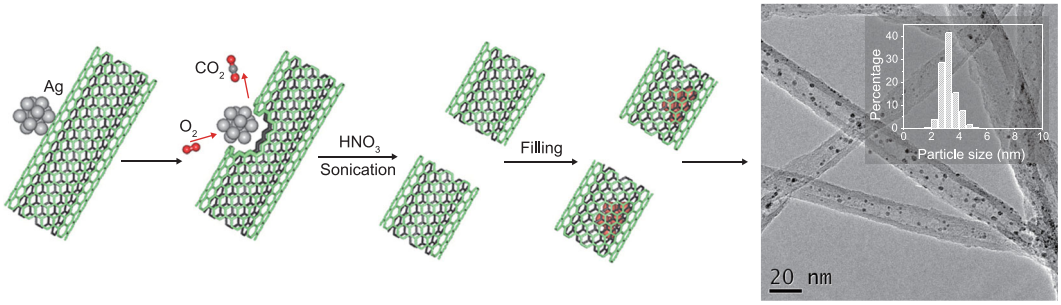

Figure 5. Scheme for efficient dispersion of NPs within CNT channels. The TEM image on the right shows Ru NPs confined in CNT; the inset shows the particle size distribution. Adapted with permission from [44].

encapsulated clusters are shifted downwards due to the strong interaction of the clusters with the interior surface of the CNTs, reflected in pronounced strain and deformation within the confined nanospace. As the effective d-band centers affect the occupancy of antibonding states of adsorbed O atoms [55,56], a lower d-band center would lead to more occupancy. This results in weaker binding of O atoms, implying that the encapsulated Fe clusters are more difficult to oxidize, while encapsulated iron oxide clusters are correspondingly easier to reduce. Such a unique confined environment also shifts the volcano-shape correlation between the catalytic activity and the dissociative binding energies of reactants, towards the metals with higher binding energies [54]. The extent of the shift can be well described by the confinement energy, which depends on the specific metals and the CNT diameters (Fig. 7).

The modified redox behavior of confined metal or metal oxide NPs can affect their catalytic activity directly, as redox reactions involve electron transfer between reactants and catalysts. For syngas conversion to liquid fuel over an iron catalyst, confined Fe nanocatalysts exhibit a much higher activity, and the yield of C_{5+} hydrocarbons is almost twice as high, compared with the same catalyst particles on the exterior of the tubes [57]. Detailed characterization reveals that the confinement facilitates formation of catalytically active iron carbide species under reaction conditions due to the modified redox behavior of confined iron (Fig. 8a and b).

Confinement is also found to enhance the catalytic activity of a bi-component RhMn catalyst in syngas conversion to C_2 oxygenates [58]. One-step synthesis of C_2 oxygenates, including the production of ethanol from syngas, remains a challenge for catalytic production of fuel. It relies on noble metals such as Ru and Rh as catalysts, but the efficiency of the process is still too low for commercialization. Our preliminary results show that this reaction benefits from confinement of RhMn NPs within CNTs, evidenced by a significantly enhanced yield of C_2 oxygenates with respect to the catalyst on the outside, because of better adsorption and dissociation of CO molecules on reduced RhMn sites (Fig. 8c and d).

Based on such systematic experimental characterization and theoretical calculations, we propose that the well-defined nanoscale channels of CNTs, with their unique electronic structure, provide an intriguing confinement environment for catalysis, which can be understood on the basis of considerations additional to the electronic confinement effects discussed above.

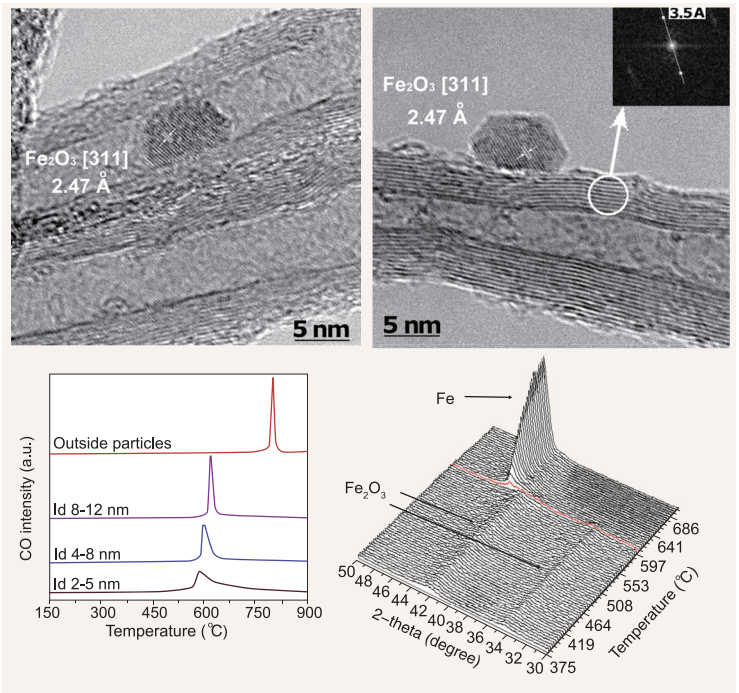

Figure 6. *In situ* HRTEM images of Fe_2O_3/CNTs at room temperature (upper), and reduction behavior of Fe_2O_3 confined in CNTs with a varying diameter, compared with that on the exterior surface (below). Adapted with permission from [52,53].

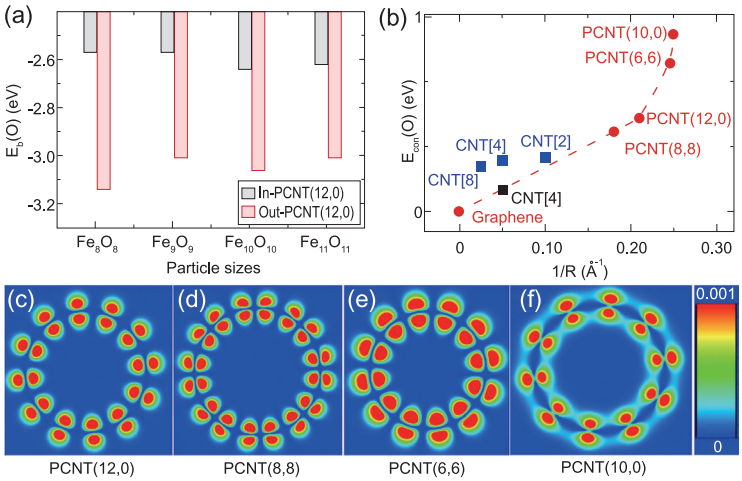

Figure 7. (a) Oxygen-binding energies, E_b(O), of Fe_nO_n ($n = 8$–11) clusters encapsulated within PCNT (12, 0) (in-PCNT) in comparison to the clusters sitting on their exterior wall (out-PCNT). (b) Confinement energy, E_{con}(O), for Fe_9O_9 clusters within PCNTs as a function of the CNT diameters, with the blue and black squares representing E_{con} estimated from the reduction of iron oxide and oxidation of metallic iron NPs within CNTs. (c–f) The electronic polarization and distribution at the valence band maximum for tubes of various inner diameters. Adapted with permission from [54].

Spatial restriction

The size and shape of NPs can be affected within the nanospace of CNTs. As a result, NPs can be dispersed there more homogeneously, with a uniform size. For example, within SWCNTs with a diameter of 1.3 nm, we have achieved dispersion of Re NPs of 0.4 nm (each consisting of around 50 metal atoms). These subnanometer-sized Re particles exhibit enhanced catalytic activity in low-temperature ammonia synthesis.

Enrichment of molecules

The nanochannels composed of sp^2 hybridized carbon exhibit hydrophobic properties, in addition to the electron-deficient environment. Thus, it can be expected that hydrophobic and nucleophilic molecules will tend to adsorb and gather inside the channels. Enrichment of hydrogen has been reported inside CNTs, stimulating wide interest in their use as hydrogen storage materials. A hydrogen storage capacity of 1.8 wt% has been reported, although the feasibility of using CNTs as efficient hydrogen storage materials has yet to be established. Our theoretical calculations show that not only H_2 but also N_2 and CO can be enriched within CNT channels. For example, at 300 K and 1 MPa, CO is enriched by 20 times within a (10,10) nanotube: in effect this means that the CO pressure within the CNT channel is enhanced by a factor of 20 in an external CO atmosphere of 1 MPa [59]. This finding might make it possible to conduct reactions that conventionally require high pressures under much milder conditions. We recently presented experimental studies on the selective enrichment of molecules with different properties in solution [60]. Our *in situ* high-resolution nuclear magnetic resonance (NMR) studies demonstrated that CNT channels can selectively absorb hydrophobic benzene relative to hydrophilic acetic acid and phenol molecules. Benzene tends to diffuse into the CNT channels, leading to locally higher concentration. Consequently, the rate of benzene conversion to phenol is enhanced 4 fold using a CNT-confined Re catalyst, relative to the same catalyst dispersed on the outer walls of the CNTs. This is not just because of local enrichment of benzene inside the CNT channels but also selective expulsion of hydrophilic phenol molecules [60]. CNT-based catalysts may thus find applications in high-pressure reactions such as the conversion of syngas to light olefins and ethylene glycol via C-C bond coupling, as well as low-pressure ammonia synthesis and some selective oxidations.

Facilitated diffusion

Transport of gas molecules in pores usually follows Knudsen diffusion via collisions with the pore walls. When the diameter of the pores is reduced to a size comparable to the dynamic diameter of confined molecules, the transport behavior of the molecules will change significantly. Extensive theoretical and experimental studies show that water molecules are transported through CNTs by a kind of 'super-diffusion' in which the molecules do not collide with the pore walls but diffuse in a form of 1D ordered chain structure held by hydrogen bonds [61]. We observed that the diffusivity of water in CNTs with an inner diameter of 2–3 nm is comparable to that in the bulk supercooled liquid [62], and is an order of magnitude higher than that reported for mesoporous silica materials with a similar pore size [63]. We recently studied methanol diffusion in multiwalled CNTs (MWCNTs), in comparison to the mesoporous silica material MCM-41, using solid-state NMR with hyperpolarized ^{129}Xe as the probe molecule. The methanol diffusion rate in MWCNTs with an inner diameter of 4 nm was estimated to be 5.4 times that inside the MCM-41 pores [64,65].

In summary, nano-confinement effects in CNTs offer opportunities for tuning the catalytic performance of metal NPs by modifying their surface structure and electronic properties without significantly changing the catalyst composition, bringing the

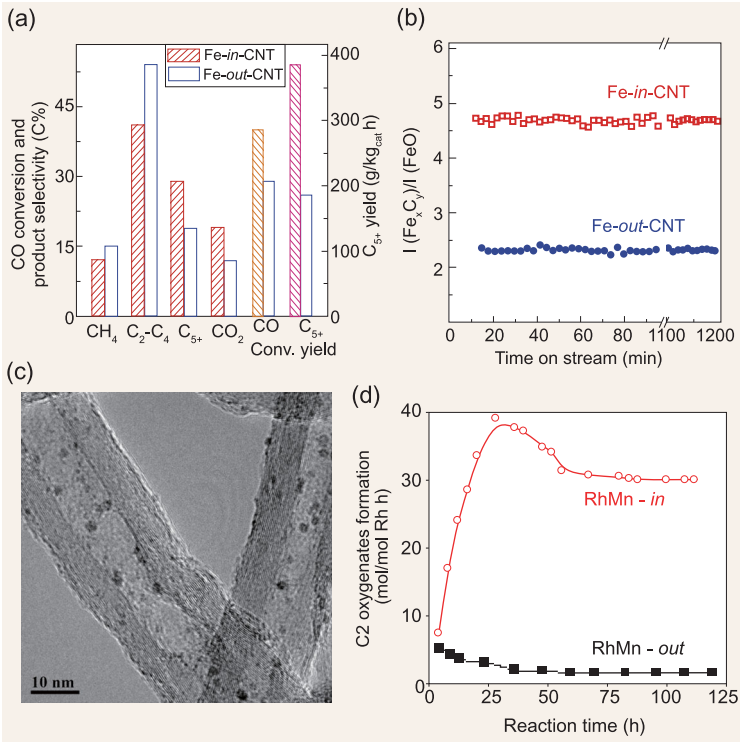

Figure 8. (a) Activity of Fe-in-CNT and Fe-outside-CNT for Fischer–Tropsch synthesis at 280°C and 50 bar. (b) Comparison of the relative ratio of iron carbide/iron oxide ratio between Fe-in-CNT and Fe-outside-CNT catalysts at 9 bar. (c) TEM image of the CNT-confined bimetallic RhMn catalyst and (d) activity of RhMn-in-CNT and RhMn-outside-CNT for syngas conversion at 320°C and 30 bar. Adapted with permission from [57,58].

rational design of catalysts from the molecular scale a step closer.

CATALYSIS OVER NANOSTRUCTURED OXIDES AND THE INTERFACE CONFINEMENT EFFECT

In enzymes, homogeneous catalysts and heterogeneous catalysts, catalytically active sites are often coordinatively unsaturated (CUS) metal sites, at which reactant molecules can adsorb and further react with each other to form products. In most cases, the active sites are composed of transition-metal cations with an intermediate valence state. This structural feature creates moderately strong bonding of reactive species with the active sites, in accordance with the Sabatier principle that the interaction between the reactants and the catalysts should be neither too strong nor too weak in order to achieve maximum activity [66].

Transition metals in the metallic state display higher reactivity to most molecules than noble metals. For example, metallic Fe atoms show much higher activity in the dissociation of O_2 than do Pt atoms. However, in many reactions involving molecular oxygen, Fe^0 atoms do not demonstrate superior catalytic performance over Pt atoms. This is because the strong interaction of Fe^0 atoms with oxygen tends to lead to the formation of stable iron oxides such as Fe_2O_3, in which the metals lose the CUS character and thus their catalytic activity. Therefore, a major challenge in catalysis is to maintain the CUS state of transition metal cations throughout the catalytic reactions. Taking Fe-based catalysts as examples, the methane monooxygenase (MMO) enzyme can convert methane to methanol under ambient conditions, and the reaction occurs on a di-iron center in which the metal atoms are typically coordinatively unsaturated [67]. In Fe-ZSM-5 zeolitic catalysts, the single iron centers are highly dispersed in the zeolite matrix, which catalyze the selective oxidation of methane at low temperatures [68]. In both catalysts, the Fe active centers have low coordination numbers and, more importantly, these sites are constrained in a nanoscale environment such as the proteins in MMO and the zeolite matrix in Fe-ZSM-5, which helps to maintain the CUS state of the Fe centers and prevent their deep oxidation during catalysis. The intrinsic interaction between the active centers and their local environment to prevent the degeneration of the CUS state is thus termed the confinement effect, which can be enforced by specific crystal structures and electronic properties of nanoscale environments, and even by the acidity/basicity of surrounding solutions.

Using oxide/metal catalytic systems, we have illustrated an interface confinement effect and its application in some catalytic systems. Heterogeneous catalysts consisting of metal NPs supported on oxides have found important applications in reactions such as selective oxidations and hydrogenations. The role of the metal/oxide interfaces is crucial in these reactions. In particular, oxygen vacancies at these interfaces, and the interaction between the metals and their oxide supports, have been regarded as the most critical factors [69,70]. These interfacial phenomena have often been explained by the concept of strong metal-support interaction introduced by Tauster *et al.* in the late 1970s [71]. In metal/oxide systems, it is hard to control the oxygen vacancies at the interface in a well-defined way and, moreover, the interfaces are buried under 3D metal NPs, making the nature of interfacial interaction difficult to control. We have deposited well-defined oxide nanostructures onto noble metal surfaces, and investigated the oxide/metal interface at the atomic and molecular level [28]. Although these so-called oxide/metal inverse catalysts were already studied

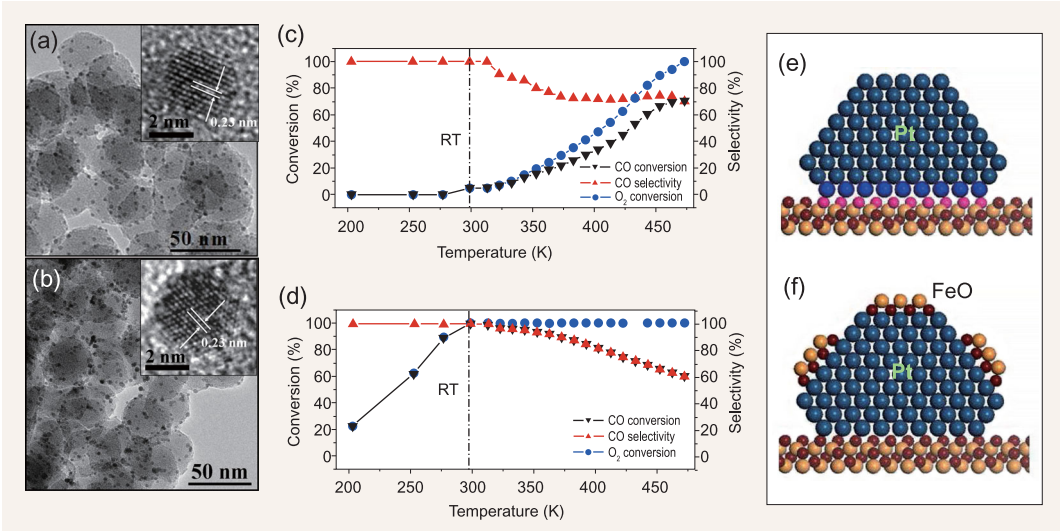

Figure 9. TEM images of the (a) Pt/SiO_2 and (b) $Pt\text{-}Fe/SiO_2$ catalysts pretreated with H_2 at 473 K for 2 h. PROX reaction of the (c) Pt/SiO_2 and (d) $Pt\text{-}Fe/SiO_2$ catalysts under the conditions of 1% CO, 0.5% O_2, and 98.5% H_2. Space velocity is 36 000 mL g^{-1} h^{-1}; pressure = 0.1 MPa. Schematics of supported Pt nanocatalyst (e) and supported Pt NP decorated by FeO nanopatches (f). Adapted with permission from [29].

in the last century [72], the recent development of *in situ* characterization techniques has allowed us to obtain deeper understanding of the oxide-metal interaction [28,73,74].

Iron oxide was deposited onto Pt surfaces to form FeO_x/Pt catalysts, in which the iron oxide is in a metastable monolayer FeO phase and the edges of the FeO islands consist of coordinatively unsaturated ferrous (CUF) sites [75]. The preferential oxidation of CO in excess of H_2 (the so-called PROX process) was chosen as the probe reaction, since PROX is often involved with noble-metal-catalyzed industrial processes and fuel-cell systems. In PROX, CO reacts selectively with O_2 to produce CO_2, rather than reacting with H_2 to form H_2O. Nowadays, the most common catalyst for this reaction consists of Pt NPs supported on SiO_2, and the CO selectivity is less than 10% at room temperature (1% CO, 0.5% O_2 and 98.5% H_2). Even at 480 K, the CO selectivity reaches only 80%, since some of O_2 molecules still react with H_2. In contrast, our $Pt\text{-}Fe/SiO_2$ catalyst delivers a performance with 100% CO conversion and 100% CO selectivity at room temperature (Fig. 9). This catalyst has been used under the working conditions of a proton electrolyte membrane fuel cell (PEMFC), which is operated at 333 K with 25% CO_2 and 20% H_2O present. By using a slight excess of O_2, CO can be removed to a level lower than 1 part per million. The catalysts were very stable, and it has been run for over 4500 h when assembled into a 1-kW PEMFC work system. We measured the oxidation state of the iron species under reaction conditions using *in situ* X-ray adsorption spectroscopy (XAFS) performed in the beamline of BL14W1 in the Shanghai Synchrotron Radiation Facility (SSRF). The results suggest the presence of ferrous species under the operating conditions [29].

Furthermore, we have constructed well-defined monolayer FeO nano-islands in the shape of triangles or hexagons on a Pt (111) surface. Both scanning tunneling microscopy (STM) and scanning tunneling spectroscopy indicate that the edges of the islands are CUF-terminated (Fig. 10), with the presence of specific CUF electronic states. We studied the surface reactivity by *in situ* ultraviolet photoelectron spectroscopy (UPS), and found that the CO-saturated Pt (111) surface is stable for O_2 exposure of 10^{-6} torr O_2 at room temperature. Under identical conditions, CO adsorbed on a 0.25 ML FeO/Pt (111) surface can be removed in five minutes by exposure to O_2. The surface reactivity is linearly dependent on the density of the FeO island edge sites, which clearly indicates that these are the active sites. DFT calculations show that at the CUF sites O_2 may either dissociate directly to atomic O without a free-energy barrier, or adsorb first in the molecular state with a binding energy of about –1.51 eV per O_2, and then dissociate afterwards to atomic O with a barrier of 0.42 eV. The dissociated O atoms have a moderate adsorption energy of –1.10 eV/O at the CUF sites, and can react quickly with CO adsorbed nearby (Fig. 11) [29].

In these highly efficient FeO/Pt catalysts, the noble metal acting as a substrate for the FeO islands not only provides surface sites for CO adsorption but

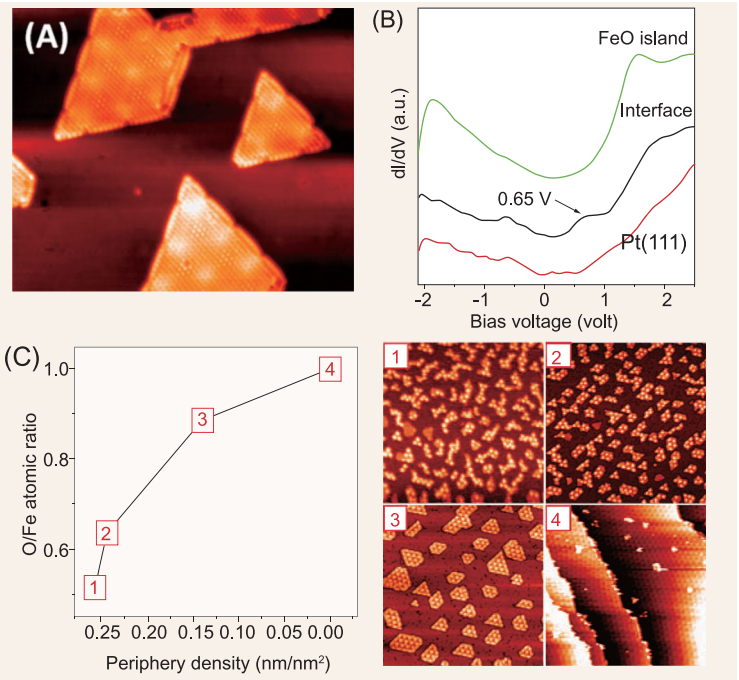

Figure 10. (A) STM image of FeO nano-islands on Pt (111) (25 nm × 20.8 nm). (B) d*I*/d*V* spectra acquired at 5 K on the surface of FeO islands, at the FeO–Pt interface, and on Pt (111). (C) Ratios of XPS O 1s to Fe $2p_{3/2}$ peak intensity from FeO/Pt (111) surfaces with different periphery density of FeO nano-islands. Samples 1–3 are 0.25 ML FeO nano-islands prepared at 1.3 × 10^{-6} mbar O_2 and annealed in UHV at 473, 573, and 673 K, respectively. Sample 4 is a full-monolayer FeO film on Pt (111). The size of STM images is all 100 nm × 100 nm. Adapted with permission from [29,75].

also exerts a constraining environment for the stabilization of the active iron centers, in a manner analogous to that in enzymes. The calculated interfacial adhesion energy is 1.40 eV per FeO formula, which originates from the strong hybridization between Pt and Fe orbitals. The interfacial metal–cation bonding prevents further oxidation of the active FeO phase to the less active FeO_{1+x} phase. Upon further oxidation, CUF sites at the edges of islands disappear, resulting in deactivation of the catalyst [76]. Based on these results, we suggested the concept of an 'interface confinement effect'.

This effect can be illustrated by the schematic diagram in Fig. 12. Again taking FeO as an example, we know that the freestanding FeO monolayer is unstable and highly reactive, and can easily dissociate O_2. There are two possible channels for the further reaction of the dissociated oxygen atoms: (1) to react with FeO, forming stable Fe_2O_3; (2) to react with CO to produce CO_2. A simple calculation suggests that the former reaction has a barrier of 0.6 eV while the latter one needs to overcome a barrier of 1.5 eV. So this susceptibility to further oxidation to Fe_2O_3 explains why a freestanding FeO monolayer cannot catalyze CO oxidation. When the FeO monolayer is placed on the Pt surface, however, the total energy is significantly lowered due to the strong interaction between FeO and Pt. The energy difference between the freestanding FeO structure and the Pt-supported FeO structure is termed the interface confinement energy ($\Delta E_{\text{confinement}}$). The energy of the FeO_{1+x} structure is much less dependent on the support. Therefore, the driving force for oxidation of the interface-confined FeO structure to the FeO_{1+x} structure is much smaller than the free structure, and a larger energy barrier for oxidation is expected according to the Brønsted-Evans-Polanyi relation [66]. In this case, CO oxidation becomes dominant. Therefore, the metal surface provides a constraining environment on which metastable FeO can remain robust in oxidative atmospheres and catalyze reactions.

The interface confinement effect is strongly dependent on the metal substrate. We have shown that the binding energy between the 2D FeO structure and the metal substrate decreases in the sequence Pt > Pd > Ru > Au > Cu > Ag. The Pt surface exhibits the strongest confinement effect on the FeO structure, while the Ag surface is weakest. The bonding of the substrate metal with Fe is critical to the interface confinement effect. The other prerequisite of a strong effect is that the metal should bind weakly with oxygen. Future work should look for other substrates, such as nanostructured carbon materials or composite materials, which can act similarly to noble metals to confine the highly active oxide nanostructures.

GRAPHENE AND 2D MATERIALS FOR CATALYSIS

Since Geim, Novoselov and coworkers reported the unique structural and electronic properties of graphene in 2004 [77], applications of graphene have attracted great attention [78]. Recently, research on the structure, properties and applications of other 2D materials such as g-C_3N_4, h-BN and MoS_2 have expanded rapidly [79,80]. The unique electronic and structural properties of 2D materials, which are easy to synthesize and control, have made them promising candidates for applications in information technologies, energy, catalysis and other fields.

2D atomic crystals consist of a single-atom layer, or alternatively a staggered multi-atom layer. Typically, atoms within the 2D plane are connected by covalent or ionic bonds, whereas the interaction between different 2D planes is dominated by van der Waals forces [81]. In graphene, the sp^2 hybridized orbitals of carbon atoms enable the sheets to exhibit excellent mechanical strength. The p orbitals,

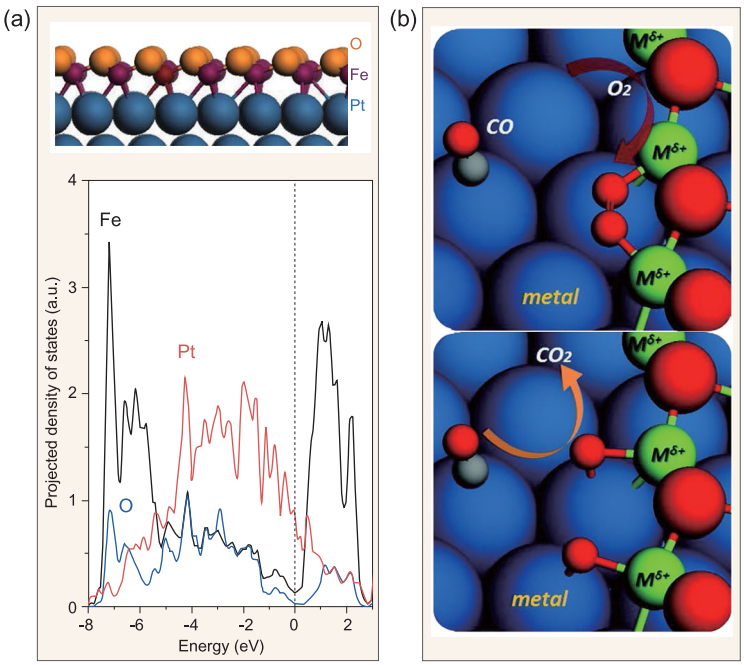

Figure 11. (a) Projected DOS for interfacial Fe, O, and Pt atoms at fcc domains of FeO overlayer on Pt (111) using ($\sqrt{84} \times \sqrt{84}$) $R10.9^\circ$ – FeO/Pt (111) supercell. (b) Schematic structures of O_2 activation and CO oxidation at the TMO/NM (111) boundaries. The initial state of O_2 adsorption (up) and the final state of O_2 dissociation (down). The blue, red, green, and gray spheres represent NM, O, 3d-TM, and C atoms, respectively. Adapted with permission from [28,29].

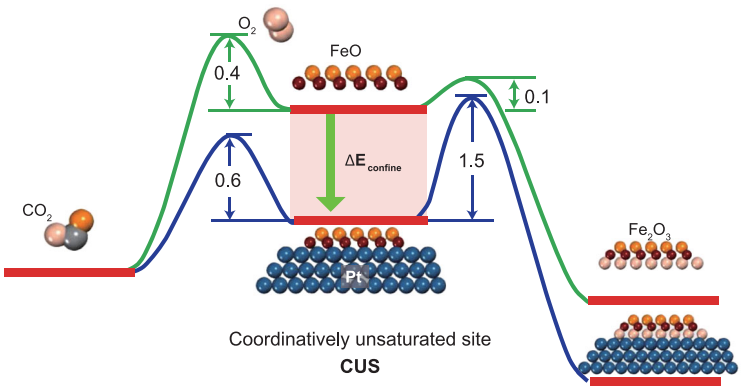

Figure 12. Schematic illustration of the interfacial confinement between Pt surface and iron oxides. The metal surface provides a constraining environment on which a metastable FeO structure can be stabilized with interfacial confinement energy $\Delta E_{confinement}$, and which remains robust during catalytic reactions in oxidative atmospheres.

perpendicular to the σ plane, form a large conjugated π bond over the entire 2D lattice, so that graphene exhibits high electrical conductivity [82]. The single-atom-layer structure of graphene also gives it a high specific surface area ($>2600\ m^2\ g^{-1}$) [83]. The valence and conduction bands intersect at a single point (the Dirac point) at the Fermi level, where there is no band gap. Therefore, graphene also shows semimetallic or zero-band semiconducting properties [84]. These electronic properties make graphene unique in its physical characteristics, with potential applications for optoelectronic devices and field-effect transistors. Its physical properties have also intrigued chemists, including researchers seeking applications in catalysis [85]. However, graphene is highly stable due to the conjugation of p orbitals over the entire atomic layer. In particular, the low density of electronic states near the Fermi level makes graphene chemically inert [86], limiting its applications in chemistry and catalysis: there is no indication that 'perfect' graphene can be used as a catalyst directly.

Previous studies [35,87,88] indicate that in order to make perfect graphene chemically active, the electronic structure must be altered by tuning the distribution of electronic states and increasing the density of states (DOS) around the Fermi level. This review describes several often used methods for improving the catalytic activity of graphene-based materials.

The preparation of nanoscale graphene sheets and the formation of structural defects on graphene

Previous studies have shown that edges or defects of graphene often exhibit enhanced reactivity due to the variety of unsaturated coordination numbers of carbon in these locations, or to functional groups attached to the carbon atoms [87,89]. Typical methods to reduce the size of graphene sheets and create defects in them are mechanical ball milling and etching. Recent reports showed varying ball-milling time and energy can control the size of graphene sheets, thereby modulating their catalytic activity for oxygen reduction reactions [87]. DFT calculations indicated that the zigzag edges can function as the active sites for such reactions regardless of whether there are oxygen-containing functional groups there. In contrast, 'armchair' edges, as well as the surface of graphene, are inert for catalysis, again with or without oxygen-containing functional groups [87]. Graphene sheets prepared by hydrothermal methods exhibit a high catalytic activity, which may originate from the high density of defects introduced at the low preparation temperatures [88].

The formation of folds on the graphene surface, resulting in distortion of the electron distribution

Folds on a graphene surface can be induced by thermal treatment, electrostatic interactions or mechanical methods [90]. During their formation, the

perfect 2D structure of graphene is destroyed, resulting in a distortion of the electronic structure at the surface. The degree of distortion depends on the radius of curvature of the folds. A typical example is the formation of bubbles under graphene [91], whereupon the strain strongly modifies the electronic properties. In principle, this method can be used for band-structure engineering of graphene and might render it suitable for catalysis.

SWCNTs may be formed by curling of graphene. The radii of curvature determine the distortion of the electron distribution inside and outside the CNTs—which is why, as discussed earlier, there are significantly different catalytic properties inside and outside CNTs [27].

Chemical modification and doping of graphene

An effective method to modify the catalytic activity of graphene is via chemical functionalization [92,93]. Hydrogen atoms terminating the edge of graphene may significantly affect the material's band gap, changing it from nearly zero at low hydrogen coverage to 3.7 eV at high coverage [94–96]. The precise effect of hydrogen is dependent on the edge structure: whether it is zigzag or armchair.

Doping is one of the most effective and common methods for the chemical modification of graphene [93,97]. The dopants used are mainly non-metallic elements such as boron, nitrogen, sulfur and phosphorus; metal atom dopants have also been reported recently. The difference in electron distribution between dopants and neighboring carbon atoms causes a local distortion of the electronic structure, thereby changing the physical and chemical (including catalytic) properties. Up to now, boron and nitrogen have been regarded as the most effective heteroatoms: these have one less and one more electron than carbon atoms, respectively. As the electronegativity of boron and nitrogen is different from carbon, they can attract electrons from or supply electrons to the surrounding carbon atoms. Nitrogen atoms tend to gain electrons from the adjacent carbon atoms because of its greater electronegativity [35,88]. Meanwhile, the lone pair electrons of nitrogen atoms feed electrons back to the surrounding carbon atoms. This synergistic effect leads to an abnormal electron distribution for carbon atoms around nitrogen atoms, increasing the electron

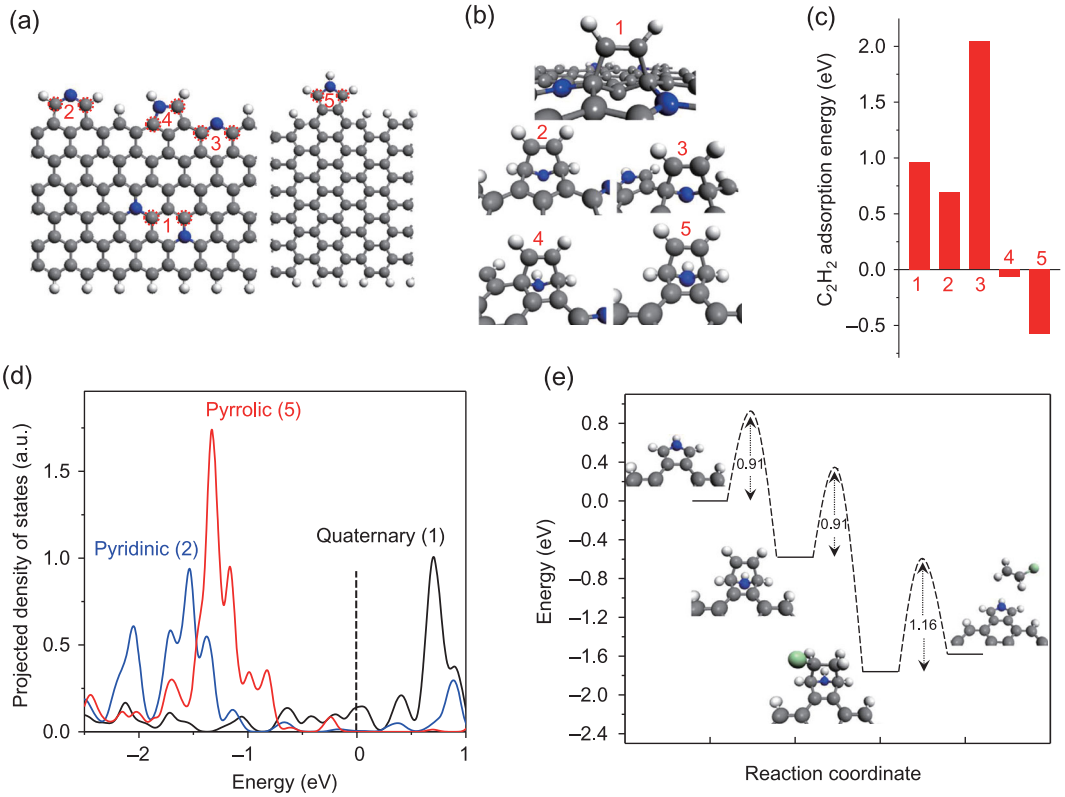

Figure 13. DFT calculations of the reaction mechanism. (a) Models with different *N* species used in the DFT calculation; the blue balls representing N atoms. (b) The structures with adsorbed C_2H_2. (c) The corresponding adsorption energies (Ea). (d) The projected density of p_z states of the C sites for C_2H_2 adsorption. (e) Reaction energy profile for acetylene hydrochlorination on the pyrrolic structure. Adapted with permission from [99].

density near the Fermi level [35,88]. In oxygen-reducing reactions, molecular oxygen preferentially interacts with these defects by dissociating, thus accelerating the reaction rate. The onset overpotential of oxygen reduction decreases with increasing concentration of nitrogen dopants. In general, nitrogen dopant atoms in graphene can form graphitic, pyridinic and pyrrolic species [98], and the nature of the catalytically active sites in nitrogen-doped graphene is still debated. Nitrogen doping of both graphene and other carbon nanostructures can yield an effective catalyst for hydrochlorination of acetylene to vinyl chloride [99]; Su *et al.* proposed that the adsorption of acetylene onto pyridinic N was the key step [100]. But extensive experimental studies by Li *et al.*, who have designed a series of model catalysts in which one or two particular types of nitrogen species dominate, suggest that pyrrolic nitrogen is the catalytic active center, a conclusion supported by DFT calculations (Fig. 13) [99]. To sum up, impurity atoms, especially nitrogen dopants, seem necessary to activate 2D carbon materials as catalysts, but the reaction mechanism awaits further clarification.

The potential application of sandwich 2D heterostructures in catalysis

Controllable methods for stacking different layers of 2D crystals in a certain order have permitted the synthesis of sandwich 2D nanomaterials with distinct heterostructures [101]. The stacked 2D layers may be bound either by van der Waals or covalent interactions, and the order and style of stacking influences the properties of the heterostructures (Fig. 14):

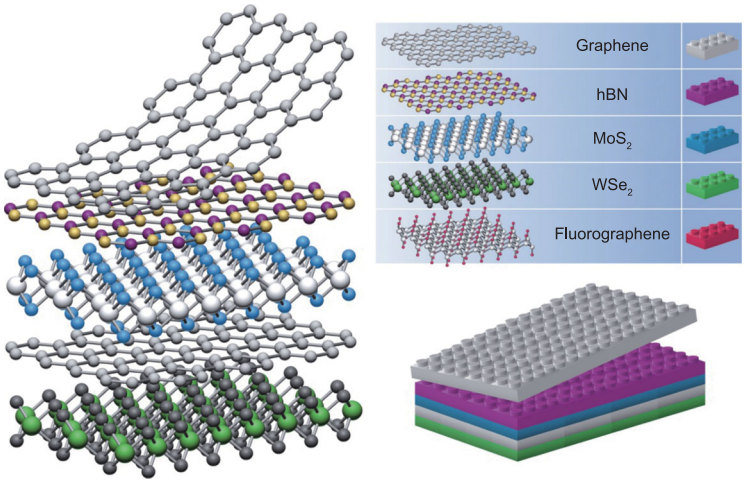

Figure 14. 2D crystals, analogous to Lego blocks (right-hand panel), are connected by van der Waals or covalent interactions between the sheets. The order and style of stacking influence the properties of these 2D heterostructures. Adapted with permission from [101].

by varying the chemical composition, structure and electronegativity of the system, the electronic property at the surfaces, interfaces or edges may be modulated drastically, resulting in properties quite different from the individual 2D materials. This creates opportunities for tuning the catalytic performance of such heterostructures, offering a new pathway for rational design and precise control. There has been rather little study of the application of sandwich 2D materials in catalysis, but a system with a similar character that has been widely studied in this context is graphite oxide: graphitic carbon with oxygen atoms inserted between the layers. The presence of the oxygen atoms can significantly alter the catalytic performance of the carbon layers [92]. Recently, there have been efforts to insert heteroatoms such as iron or noble metals into graphite oxide to modulate its catalytic performance: this approach could prove of great interest.

In the past decade, we have performed systematic studies of catalysis of 2D atomic crystals, including graphene, MoS_2 and BN. We have identified a confinement effect for reactions occurring between the layers, or at the interface of such 2D materials and a metal substrate. In particular, we have observed enhanced catalytic performance of graphene-encapsulated metal NPs, due to the penetration of electrons from the metals into the covering graphene sheet. We have elaborated the principles that we call 'catalysis under graphitic cover' [102] and 'chainmail for catalysts'.

Catalysis under the cover of graphene

Graphene overlayers interact with most metals via the van der Waals force; the distance between the graphene cover sheet and the substrate surface is typically 0.3–1.0 nm. Therefore, the space at the graphene/metal interface can be regarded as a 2D nanocontainer, in which atoms and molecules can be trapped. It has been shown that Si, Ni, Pb and noble metals can intercalate into graphene grown on metal surfaces [103–107]. A comparative study of the intercalation process revealed that it may happen through an exchange mechanism or a defect-aided mechanism, depending on the interaction strength of the intercalants with graphene [105]. For example, Ni, Fe and Si, which interact with carbon strongly, can produce transient defects at the graphene lattice and penetrate into the interface via exchange between surface metal atoms and carbon atoms at the transient defect sites. In contrast, Pb and Au bond weakly with carbon, and the intercalation of these elements needs to be facilitated by extended defects such as graphene island edges, domain boundaries and large vacancies.

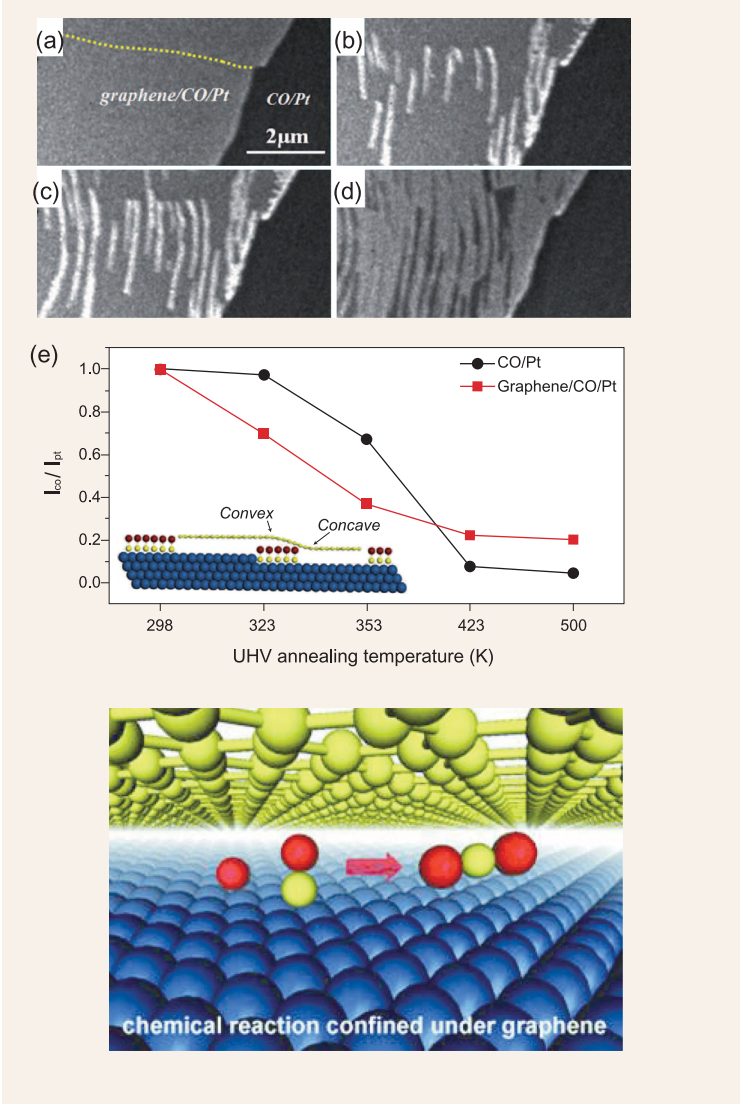

Figure 15. (a–d) Low-energy electron microscopy (LEEM) images recording CO intercalation at the graphene/Pt (111) interface in 1×10^{-6} mbar CO at room temperature. (e) XPS O 1s intensity of a CO-saturated Pt (111) surface and CO-intercalated 0.7 ML graphene/Pt (111) surface annealed at various temperatures in ultra-high vacuum (UHV). The schematic illustration of the chemical reaction under the cover of graphene (below). Adapted with permission from [113].

The intercalation of molecules such as CO, O_2 and H_2O under the graphene surface should be facilitated by the defect-aided intercalation mechanism [108–113]. The driving force of this process is the strong adsorption of the molecules onto metal surfaces. The intercalated molecules interact simultaneously with the metal and with the graphene cover, and are thus strongly confined in the direction normal to the surface. For instance, CO adsorption on Pt and Ru surfaces is greatly weakened by a graphene overlayer, due to confinement by the layer [113,114]. The space between graphene and Pt then acts as a 2D confining nanoreactor in which catalytic reactions are promoted. We have shown that while the reaction barrier of CO oxidation on Pt (111) is 0.74 eV, at the interface of Pt with a graphene overlayer it has a smaller barrier of 0.56 eV (Fig. 15) [115]. This cover effect on metal-catalyzed reactions has been found also with h-BN and MoS_2. These findings may suggest a new avenue for modulating the catalytic performance of metal catalysts.

Chainmail for catalysts

In ancient combat, for protection against blades soldiers often wore chainmail. Ideally, this not only protected the body but also did not hinder the fighting capacity of the soldier. We have shown that graphene or other nanocarbon structures can satisfy analogous requirements for metal catalysts.

Previous studies have shown that iron catalysts–especially iron in low valence states–exhibit high catalytic activities for reactions such as oxygen-reduction reactions (ORR) in fuel cells [116]. However, the iron is easily oxidized to its high valence state and thus deactivated. Furthermore, the active iron components are likely to corrode under the acidic conditions of fuel cells.

To solve these problems, we have designed an efficient synthesis method to encapsulate iron NPs into CNTs to avoid direct contact of iron with oxygen molecules, with the acidic solution and with some possible poisons during the reaction process [117]: to give the highly active NPs protective 'chainmail' against the harsh environment while permitting the electrons of the encapsulated metal to 'penetrate' through the carbon layer and reach the external surface of the graphene shell. These electrons increase the DOS near the Fermi level of the external carbon atoms, decreasing their local work function (Fig. 16) [117–119]. This promotes the adsorption and dissociation of oxygen molecules on the graphene shell, thereby maintaining or even enhancing the catalytic ORR activity of the iron NPs. The catalyst obtained by this strategy showed excellent activity and stability when adopted as the cathode catalyst in the real fuel cells; even after 200 h of operation under acidic conditions, the cell's efficiency showed no obvious degradation. Furthermore, the catalyst showed no decline in performance in the presence of 10 ppm SO_2, thereby exhibiting superior anti-acid and sulfur-poisoning-resistant properties relative to commercial Pt/C catalysts (Fig. 17) [117].

Theoretical and experimental studies on this system [120–124] have shown that the composition of the encapsulated metals or metal alloys, the thickness of carbon layers and the concentration of nitrogen dopants in these layers are the key factors

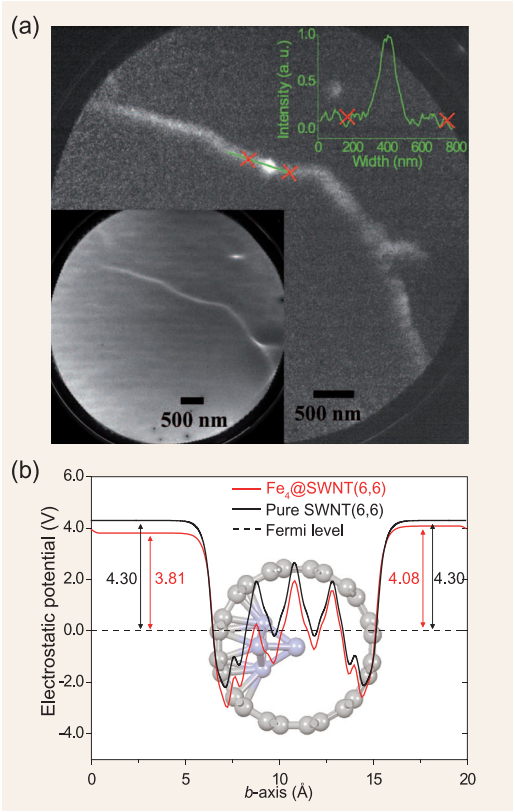

Figure 16. (a) Photoemission electron microscopy image of Fe clusters encapsulated in a pod-like CNT, with a laser start voltage of 1.7 V. The top inset showing the brightness profile along the green line. The bottom inset showing the corresponding LEEM image of the same region. (b) The electrostatic potential profiles averaged on the plane perpendicular to *b*-axis as a function of the *b*-axis of the supercell of Fe_4@SWNT and pure SWNT, respectively. The structure of Fe_4@SWNT is shown in the background. SWNT: single-wall nanotubes. Adapted with permission from [117].

influencing catalytic performance [118,123]. The latest results showed that a FeCo alloy encapsulated in nitrogen-doped graphene (average 4 layers) can provide a maximum power density of 328 mW cm^{-2} for a fuel cell operating at 80°C, with no obvious degradation of performance over 150 h. DFT calculations suggested that decreasing the number of graphene layers and increasing the nitrogen-dopant concentration would enhance the catalytic activity further [118]. And in fact, when the layer number of graphene is reduced to only 1–3 layers, the catalytic activity at the outer surface of the graphene shell is enhanced enormously; the activity of encapsulated CoNi catalysts for hydrogen evolution reaction is then very close to that of commercial 40% Pt/C catalysts (Fig. 18) [123]. This strategy of 'chain-mail' coating of particles in 2D materials thus paves the way for rational design of non-precious metal catalysts.

FUTURE PERSPECTIVES IN NANO-CATALYSIS

In summary, nanotechnology can in principle provide an effective and quantitative way to tailor the surface structures and electronic properties of supported nanocatalysts without changing their composition. However, to achieve this goal, there are still difficult challenges for both fundamental and applied research.

The controlled preparation of catalytic nanomaterials and the rational design of catalytic active centers

The controlled fabrication of nanomaterials of specific composition and structure is vital for catalytic applications. Despite the great successes so far, there are still challenges in correlating the structures of nanomaterials with their catalytic properties, hindering rational design of catalytic active centers from first principles. The first major challenge is to synthesize identical nanostructures. Current accuracy in size control of NPs has reached the sub-nanometer level, but individual NP may still differ in the numbers of atoms they contain by hundreds or even thousands. Moreover, control of the surface structure and the distribution of defects remain extremely difficult. And while it is now easy to prepare various forms of CNTs, selective synthesis with precise control of the number of wall layers, metallic or semiconducting properties, and the amount or distribution of dopants such as N and B remains very difficult, yet is critical to the catalytic activity of nanotube-based materials.

The second major challenge is to understand the dynamics of catalytic nanostructures. Catalysis is, in general, a dynamic process, which often occurs at high temperatures, under high pressures, and in the presence of a variety of reactants and products. Under such harsh conditions, NPs are expected to be 'sensitive', undergoing pronounced changes in their composition, structure and electronic state. These dynamic changes might, to some extent, be similar to those found in biological catalytic processes. It is of tremendous importance to correlate the static structures of active centers with their dynamic structures.

The *in situ* characterization of catalysts and catalytic processes

Current state-of-the-art characterization techniques have been able to probe catalytic systems at the nanometer or even sub-nanometer scale, with time intervals of nanoseconds or even femtoseconds and an energy resolution ranging from μeV to meV. However, it remains a major challenge to apply

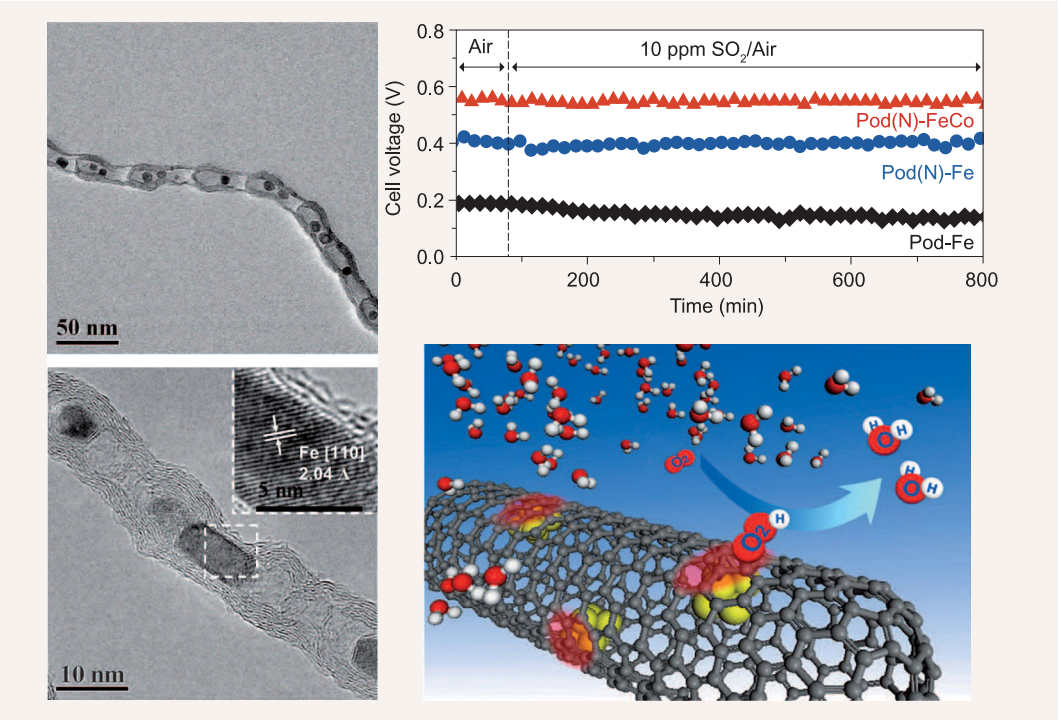

Figure 17. Iron encapsulated within pod-like CNTs for an oxygen reduction reaction, and a schematic representation of the process at the surface of Fe_4@SWNT. The gray C, red O, white H and yellow Fe atoms. Adapted with permission from [117].

these techniques for characterizing catalysts under the temperature and pressure conditions at which catalysis actually happens: electron probes are difficult to operate under high pressures, for instance. A second problem is the damaging effects of probe particles such as electrons and ions: these usually carry high energies and can cause severe deterioration of the catalytic system being probed, distorting their true nature. Recent research has focused on the development and use of techniques that are compatible with real catalytic conditions, such as photon-in/photon-out, electromagnetic and microwave methods. At synchrotron radiation sources, the use of an X-ray beam together with high-intensity infrared (IR) beam focused on the same spot or region of a sample would permit the combination of XAFS with FT-IR measurements. Since both techniques have high time resolution, one could in principle measure simultaneously the electronic properties of catalysts using XAFS, structural information using XAFS, and chemical and bonding information of adsorbates and intermediates using high-resolution FT-IR, with a temporal resolution at the μs or ms level. This would enable a dynamic picture of the *in situ* catalytic process to be constructed under realistic reaction conditions of high temperatures and pressures.

Computational chemistry approximating the complexity of experiments

The rapid development of computational chemistry has enabled us to simulate nanomaterials and reaction systems with relatively high precision. Currently, it is not very difficult to perform calculations for a model system with more than 1000 atoms using optimized DFT methods. However, for catalytic reactions, *ab initio* calculations of large systems interacting with their chemical environment remain highly challenging. The development of new theoretical methods to analyze individual elementary catalytic steps involving adsorption, desorption, diffusion and reaction, and to clarify the evolution of electronic properties at each step, would be tremendously valuable. Here, dialogue between theorists and experimentalists is essential. Real catalytic systems are complex in ways that current computing methods cannot sufficiently capture. Experimental insights can therefore contribute to improvements in theoretical methods and strategies. Conversely, experimentalists can optimize their methods by exploiting insights from theoretical calculations. Right now, predictive catalysis using purely theoretical simulations remains out of reach.

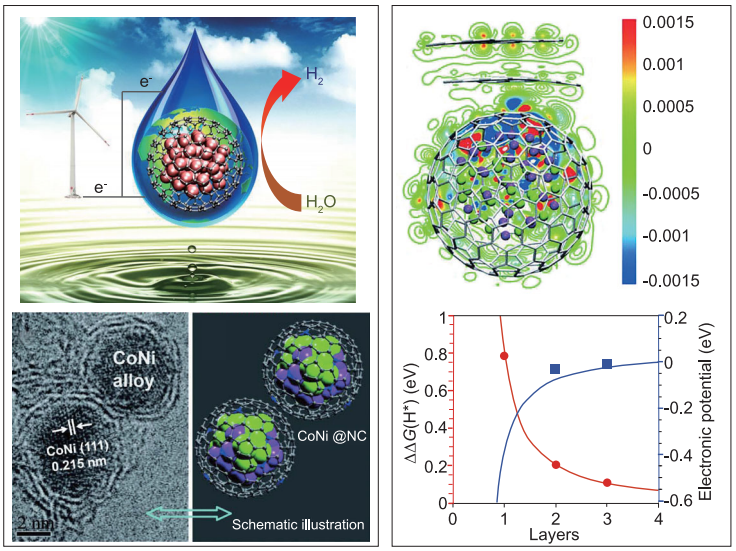

Figure 18. Enhanced catalytic performance of metals encapsulated with 2D crystals due to electron transfer between the two materials. There is a strong layer dependence of electron transfer from the metals to the outside surface of 2D crystals: reducing the number of layers in the 2D crystals significantly promotes the electron transfer and enhances the catalytic activity. Adapted with permission from [123].

The scale-up and commercialization of nanocatalysts

Catalysis is a scientific discipline with a strongly applied orientation. The results of catalytic research should ultimately lead to the design of catalysts with high performance and catalytic processes with high efficiency. There are many important issues that need be solved in the commercialization of nanocatalysts, such as their synthesis and stability under industrial reaction conditions, and the regeneration and recycling of deactivated catalysts. Due to the high hydrophobicity of NPs, nanocatalysts are usually difficult to shape and process. With a view to developing nitrogen-doped graphene nanosheets for the practical hydrochlorination of acetylene, we recently developed a method for growing them directly on the surfaces of pre-formed SiC particles by chemical etching and thermal splitting. In this way, we have successfully synthesized the catalysts in a manner that is suitable for industrial applications [99].

In summary, we can expect nanotechnology to play an increasingly important role in catalysis, making the design of highly efficient catalysts feasible at the molecular scale.

FUNDING

This work was supported by the 'Strategic Priority Research Program' of the Chinese Academy of Sciences (XDA09030101), the 'Key Research Program' of the Chinese Academy of Sciences (KGZD-EW-T05), the Ministry of Science and Technology of China (2013CB933100), the National Natural Science Foundation of China (21321002, 21425312, 21303191, 21303195, 21473191).

REFERENCES

1. Ertl, G, Knozinger, H and Schuth, F *et al. Handbook of Heterogeneous Catalysis*. Weinheim: Wiley-VCH, 1997.
2. Somorjai, GA, Contreras, AM and Montano, M *et al.* Clusters, surfaces, and catalysis. *Proc Natl Acad Sci USA* 2006; **103**: 10577–83.
3. Nilsson, A, Pettersson, LG and Norskov, J. *Chemical Bonding at Surfaces and Interfaces*. Amsterdam: Elsevier, 2008.
4. Anderson, JR and Boudart, M. *Catalysis Science and Technology*. New York: Springer, 1987.
5. Thomas, J and Thomas, W. *Principles and Practice of Heterogeneous Catalysis*. Weinheim: Wiley-VCH, 1997.
6. Ertl, G. Heterogeneous catalysis on the atomic scale. *Chem Rec* 2001; **1**: 33–45.
7. Gates, BC. *Catalytic Chemistry*. New York: Wiley, 1992.
8. Somorjai, GA. *Introduction to Surface Chemistry and Catalysis*. New York: Wiley, 1994.
9. Chorkendorff, I and Niemantsverdriet, JW. *Concepts of Modern Catalysis and Kinetics*. Weinheim: Wiley-VCH, 2003.
10. Ertl, G. Surface science and catalysis—studies on the mechanism of ammonia synthesis: the P. H. Emmett award address. *Catal Rev Sci Eng* 1980; **21**: 201–23.
11. Spencer, N, Schoonmaker, R and Somorjai, G. Iron single crystals as ammonia synthesis catalysts: effect of surface structure on catalyst activity. *J Catal* 1982; **74**: 129–35.
12. Greeley, J, Nørskov, JK and Mavrikakis, M. Electronic structure and catalysis on metal surfaces. *Annu Rev Phys Chem* 2002; **53**: 319–48.
13. Bell, AT. The impact of nanoscience on heterogeneous catalysis. *Science* 2003; **299**: 1688–91.
14. Schlögl, R and Abd Hamid, SB. Nanocatalysis: mature science revisited or something really new? *Angew Chem Int Ed* 2004; **43**: 1628–37.
15. Vajda, S, Pellin, MJ and Greeley, JP *et al.* Subnanometre platinum clusters as highly active and selective catalysts for the oxidative dehydrogenation of propane. *Nat Mater* 2009; **8**: 213–6.
16. Yamamoto, K, Imaoka, T and Chun, W-J *et al.* Size-specific catalytic activity of platinum clusters enhances oxygen reduction reactions. *Nat Chem* 2009; **1**: 397–402.
17. Haruta, M, Kobayashi, T and Sano, H *et al.* Novel gold catalysts for the oxidation of carbon monoxide at a temperature far below 0°C. *Chem Lett* 1987; **16**: 405–8.
18. Lei, Y, Mehmood, F and Lee, S *et al.* Increased silver activity for direct propylene epoxidation via subnanometer size effects. *Science* 2010; **328**: 224–8.
19. Thomas, JM. *Design and Applications of Single-site Heterogeneous Catalysts—Contributions to Green Chemistry, Clean Technology and Sustainability*. London: Imperial College Press, 2012.

20. Valden, M, Lai, X and Goodman, DW. Onset of catalytic activity of gold clusters on titania with the appearance of nonmetallic properties. *Science* 1998; **281**: 1647–50.
21. Ma, X, Jiang, P and Qi, Y *et al.* Experimental observation of quantum oscillation of surface chemical reactivities. *Proc Natl Acad Sci USA* 2007; **104**: 9204–8.
22. Haruta, M and Daté, M. Advances in the catalysis of Au nanoparticles. *Appl Catal A* 2001; **222**: 427–37.
23. Xie, X, Li, Y and Liu, Z-Q *et al.* Low-temperature oxidation of CO catalysed by Co_3O_4 nanorods. *Nature* 2009; **458**: 746–9.
24. Wei, HS, Liu, XY and Wang, AQ *et al.* FeO_x-supported platinum single-atom and pseudo-single-atom catalysts for chemoselective hydrogenation of functionalized nitroarenes. *Nat Commun* 2014; **5**: 5634.
25. Yang, XF, Wang, A and Qiao, B *et al.* Single-atom catalysts: a new frontier in heterogeneous catalysis. *Acc Chem Res* 2013; **46**: 1740–8.
26. Sun, J, Ma, D and Zhang, H *et al.* Toward monodispersed silver nanoparticles with unusual thermal stability. *J Am Chem Soc* 2006; **128**: 15756–64.
27. Pan, XL and Bao, XH. The effects of confinement inside carbon nanotubes on catalysis. *Acc Chem Res* 2011; **44**: 553–62.
28. Fu, Q, Yang, F and Bao, X. Interface-confined oxide nanostructures for catalytic oxidation reactions. *Acc Chem Res* 2013; **46**: 1692–701.
29. Fu, Q, Li, W-X and Yao, Y *et al.* Interface-confined ferrous centers for catalytic oxidation. *Science* 2010; **328**: 1141–4.
30. Serp, P and Machado, B. *Nanostructured Carbon Materials for Catalysis*. Cambridge: Royal Society of Chemistry, 2015.
31. Su, D. Nanostructured carbon for catalysis. Beijing: Science Press, 2014.
32. Mestl, G, Maksimova, NI and Keller, N *et al.* Carbon nanofilaments in heterogeneous catalysis: an industrial application for new carbon materials? *Angew Chem Int Ed* 2001; **40**: 2066–8.
33. Yu, L, Li, WX and Pan, XL *et al.* In- and out-dependent interactions of iron with carbon nanotubes. *J Phys Chem C* 2012; **116**: 16461–6.
34. Haddon, RC. Chemistry of the fullerenes: the manifestation of strain in a class of continuous aromatic molecules. *Science* 1993; **261**: 1545–50.
35. Yu, L, Pan, X and Cao, X *et al.* Oxygen reduction reaction mechanism on nitrogen-doped graphene: a density functional theory study. *J Catal* 2011; **282**: 183–90.
36. Serp, P and Castillejos, E. Catalysis in carbon nanotubes. *ChemCatChem* 2010; **2**: 41–7.
37. Pan, XL and Bao, XH. Reactions over catalysts confined in carbon nanotubes. *Chem Commun* 2008: 6271–81.
38. Su, DS, Perathoner, S and Centi, G. Nanocarbons for the development of advanced catalysts. *Chem Rev* 2013; **113**: 5782–816.
39. Ajayan, PM and Iijima, S. Capillarity-induced filling of carbon nanotubes. *Nature* 1993; **361**: 333–4.
40. Guerret-Piecourt, C, Lebouar, Y and Loiseau, A *et al.* Relation between metal electronic structure and morphology of metal compounds inside carbon nanotubes. *Nature* 1994; **372**: 761–5.
41. Ugarte, D, Chatelain, A and de Heer, WA. Nanocapillarity and chemistry in carbon nanotubes. *Science* 1996; **274**: 1897–9.
42. Castillejos, E, Debouttiere, P-J and Roiban, L *et al.* An efficient strategy to drive nanoparticles into carbon nanotubes and the remarkable effect of confinement on their catalytic performance. *Angew Chem Int Ed* 2009; **48**: 2529–33.
43. Tessonnier, J-P, Ersen, O and Weinberg, G *et al.* Selective deposition of metal nanoparticles inside or outside multi-walled carbon nanotubes. *ACS Nano* 2009; **3**: 2081–9.
44. Wang, CF, Guo, SJ and Pan, XL *et al.* Tailored cutting of carbon nanotubes and controlled dispersion of metal nanoparticles inside their channels. *J Mater Chem* 2008; **18**: 5782–6.
45. Zhang, F, Pan, XL and Hu, YF *et al.* Tuning the redox activity of encapsulated metal clusters via the metallic and semiconducting character of carbon nanotubes. *Proc Natl Acad Sci USA* 2013; **110**: 14861–6.
46. Zhang, HB, Pan, XL and Liu, JY *et al.* Enhanced catalytic activity of subnanometer titania clusters confined inside double-wall carbon nanotubes. *ChemSusChem* 2011; **4**: 975–80.
47. Zhang, H, Pan, X and Bao, X. Facile filling of metal particles in small carbon nanotubes for catalysis. *J Energy Chem* 2013; **22**: 251–6.
48. Golberg, D, Gu, CZ and Bando, Y *et al.* Peculiarities of Fe–Ni alloy crystallization and stability inside C nanotubes as derived through electron microscopy. *Acta Mater* 2005; **53**: 1583–93.
49. Kondratyuk, P and Yates, JT, Jr. Molecular views of physical adsorption inside and outside of single-wall carbon manotubes. *Acc Chem Res* 2007; **40**: 995–1004.
50. Li, LJ, Khlobystov, AN and Wiltshire, JG *et al.* Diameter-selective encapsulation of metallocenes in single-walled carbon nanotubes. *Nat Mater* 2005; **4**: 481–5.
51. Sloan, J, Wright, DM and Woo, HG *et al.* Capillarity and silver nanowire formation observed in single walled carbon nanotubes. *Chem Commun* 1999: 699–700.
52. Chen, W, Pan, XL and Willinger, MG *et al.* Facile autoreduction of iron oxide/carbon nanotube encapsulates. *J Am Chem Soc* 2006; **128**: 3136–7.
53. Chen, W, Pan, XL and Bao, XH. Tuning of redox properties of iron and iron oxides via encapsulation within carbon nanotubes. *J Am Chem Soc* 2007; **129**: 7421–6.
54. Xiao, JP, Pan, XL and Guo, SJ *et al.* Toward fundamentals of confined catalysis in carbon nanotubes. *J Am Chem Soc* 2015; **137**: 477–82.
55. Hammer, B and Norskov, JK. Why gold is the noblest of all the metals. *Nature* 1995; **376**: 238–40.
56. Mavrikakis, M, Hammer, B and Norskov, JK. Effect of strain on the reactivity of metal surfaces. *Phys Rev Lett* 1998; **81**: 2819–22.
57. Chen, W, Fan, ZL and Pan, XL *et al.* Effect of confinement in carbon nanotubes on the activity of Fischer-Tropsch iron catalyst. *J Am Chem Soc* 2008; **130**: 9414–9.
58. Pan, XL, Fan, ZL and Chen, W *et al.* Enhanced ethanol production inside carbon-nanotube reactors containing catalytic particles. *Nat Mater* 2007; **6**: 507–11.
59. Guan, J, Pan, XL and Liu, X *et al.* Syngas segregation induced by confinement in carbon nanotubes: a combined first-principles and Monte Carlo study. *J Phys Chem C* 2009; **113**: 21687–92.
60. Zhang, HB, Pan, XL and Han, XW *et al.* Enhancing chemical reactions in a confined hydrophobic environment: an NMR study of benzene hydroxylation in carbon nanotubes. *Chem Sci* 2013; **4**: 1075–8.
61. Hummer, G, Rasaiah, JC and Noworyta, JP. Water conduction through the hydrophobic channel of a carbon nanotube. *Nature* 2001; **414**: 188–90.
62. Gillen, KT, Douglass, DC and Hoch, JR. Self-diffusion in liquid water to −31°C. *J Chem Phys* 1972; **57**: 5117–9.
63. Liu, X, Pan, XL and Zhang, SM *et al.* Diffusion of water inside carbon nanotubes studied by pulsed field gradient NMR spectroscopy. *Langmuir* 2014; **30**: 8036–45.
64. Zhang, C, Zhu, W and Li, S *et al.* Sintering-resistant Ni-based reforming catalysts obtained via the nanoconfinement effect. *Chem Commun* 2013; **49**: 9383–5.

65. Yue, H, Zhao, Y and Zhao, S *et al.* A copper-phyllosilicate core-sheath nanoreactor for carbon–oxygen hydrogenolysis reactions. *Nat Commun* 2013; **4**: 2339.
66. Bligaard, T, Nørskov, JK and Dahl, S *et al.* The Brønsted–Evans–Polanyi relation and the volcano curve in heterogeneous catalysis. *J Catal* 2004; **224**: 206–17.
67. Merkx, M, Kopp, DA and Sazinsky, MH *et al.* Dioxygen activation and methane hydroxylation by soluble methane monooxygenase: a tale of two irons and three proteins. *Angew Chem Int Ed* 2001; **40**: 2782–807.
68. Panov, GI, Uriarte, AK and Rodkin, MA *et al.* Generation of active oxygen species on solid surfaces. Opportunity for novel oxidation technologies over zeolites. *Catal Today* 1998; **41**: 365–85.
69. Fu, Q and Wagner, T. Interaction of nanostructured metal overlayers with oxide surfaces. *Surf Sci Rep* 2007; **62**: 431–98.
70. Campbell, CT. Ultrathin metal films and particles on oxide surfaces: structural, electronic and chemisorptive properties. *Surf Sci Rep* 1997; **27**: 1–111.
71. Tauster, S, Fung, S and Garten, R. Strong metal-support interactions. Group 8 noble metals supported on titanium dioxide. *J Am Chem Soc* 1978; **100**: 170–5.
72. Schwab, G-M. Electronics of supported catalysts. *Adv Catal* 1979; **27**: 1–22.
73. Surnev, S, Fortunelli, A and Netzer, FP. Structure–property relationship and chemical aspects of oxide–metal hybrid nanostructures. *Chem Rev* 2012; **113**: 4314–72.
74. Senanayake, SD, Stacchiola, D and Rodriguez, JA. Unique properties of ceria nanoparticles supported on metals: novel inverse ceria/copper catalysts for CO oxidation and the water-gas shift reaction. *Acc Chem Res* 2013; **46**: 1702–11.
75. Yao, Y, Fu, Q and Wang, Z *et al.* Growth and characterization of two-dimensional FeO nanoislands supported on Pt (111). *J Phys Chem C* 2010; **114**: 17069–79.
76. Fu, Q, Yao, Y and Guo, X *et al.* Reversible structural transformation of FeO_x nanostructures on Pt under cycling redox conditions and its effect on oxidation catalysis. *Phys Chem Chem Phys* 2013; **15**: 14708–14.
77. Novoselov, KS, Geim, AK and Morozov, SV *et al.* Electric field effect in atomically thin carbon films. *Science* 2004; **306**: 666–9.
78. Allen, MJ, Tung, VC and Kaner, RB. Honeycomb carbon: a review of graphene. *Chem Rev* 2010; **110**: 132–45.
79. Castro Neto, AH and Novoselov, K. Two-dimensional crystals: beyond graphene. *Mater Express* 2011; **1**: 10–7.
80. Deng, J, Li, H and Xiao, J *et al.* Triggering the electrocatalytic hydrogen evolution activity of the inert two-dimensional MoS_2 surface via single-atom metal doping. *Energy Environ Sci* 2015, doi: 10.1039/C5EE00751H.
81. Novoselov, KS, Jiang, D and Schedin, F *et al.* Two-dimensional atomic crystals. *Proc Natl Acad Sci USA* 2005; **102**: 10451–3.
82. Geim, AK and Novoselov, KS. The rise of graphene. *Nat Mater* 2007; **6**: 183–91.
83. Chae, HK, Siberio-Perez, DY and Kim, J *et al.* A route to high surface area, porosity and inclusion of large molecules in crystals. *Nature* 2004; **427**: 523–7.
84. Castro Neto, AH, Guinea, F and Peres, NMR *et al.* The electronic properties of graphene. *Rev Mod Phys* 2009; **81**: 109–62.
85. Ruoff, R. Graphene: calling all chemists. *Nat Nanotechnol* 2008; **3**: 10–1.
86. Deng, D, Pan, X and Zhang, H *et al.* Freestanding graphene by thermal splitting of silicon carbide granules. *Adv Mater* 2010; **22**: 2168–71.
87. Deng, D, Yu, L and Pan, X *et al.* Size effect of graphene on electrocatalytic activation of oxygen. *Chem Commun* 2011; **47**: 10016–8.
88. Deng, D, Pan, X and Yu, L *et al.* Toward N-doped graphene via solvothermal synthesis. *Chem Mater* 2011; **23**: 1188–93.
89. Zhang, J, Liu, X and Blume, R *et al.* Surface-modified carbon nanotubes catalyze oxidative dehydrogenation of n-butane. *Science* 2008; **322**: 73–7.
90. Chae, SJ, Guenes, F and Kim, KK *et al.* Synthesis of large-area graphene layers on poly-nickel substrate by chemical vapor deposition: wrinkle formation. *Adv Mater* 2009; **21**: 2328–33.
91. Chen, CM, Zhang, Q and Huang, CH *et al.* Macroporous 'bubble' graphene film via template-directed ordered-assembly for high rate supercapacitors. *Chem Commun* 2012; **48**: 7149–51.
92. Dreyer, DR, Park, S and Bielawski, CW *et al.* The chemistry of graphene oxide. *Chem Soc Rev* 2010; **39**: 228–40.
93. Kong, XK, Chen, CL and Chen, QW. Doped graphene for metal-free catalysis. *Chem Soc Rev* 2014; **43**: 2841–57.
94. Elias, DC, Nair, RR and Mohiuddin, TMG *et al.* Control of graphene's properties by reversible hydrogenation: evidence for graphane. *Science* 2009; **323**: 610–3.
95. Sofo, JO, Chaudhari, AS and Barber, GD. Graphane: a two-dimensional hydrocarbon. *Phys Rev B* 2007; **75**: 153401.
96. Bang, J, Meng, S and Sun, Y-Y *et al.* Regulating energy transfer of excited carriers and the case for excitation-induced hydrogen dissociation on hydrogenated graphene. *Proc Natl Acad Sci USA* 2013; **110**: 908–11.
97. Li, X, Pan, X and Bao, X. Nitrogen doped carbon catalyzing acetylene conversion to vinyl chloride. *J Energy Chem* 2014; **23**: 131–5.
98. Wei, DC, Liu, YQ and Wang, Y *et al.* Synthesis of N-doped graphene by chemical vapor deposition and its electrical properties. *Nano Lett* 2009; **9**: 1752–8.
99. Li, XY, Pan, XL and Yu, L *et al.* Silicon carbide-derived carbon nanocomposite as a substitute for mercury in the catalytic hydrochlorination of acetylene. *Nat Commun* 2014; **5**: 3688.
100. Zhou, K, Li, B and Zhang, Q *et al.* The catalytic pathways of hydrohalogenation over metalfree nitrogen-doped carbon nanotubes. *ChemSusChem* 2014; **7**: 723–8.
101. Geim, AK and Grigorieva, IV. Van der Waals heterostructures. *Nature* 2013; **499**: 419–25.
102. Fu, Q and Bao, X. Catalysis on a metal surface with a graphitic cover. *Chin J Catal* 2015; **36**: 517–9.
103. Huang, L, Pan, Y and Pan, L *et al.* Intercalation of metal islands and films at the interface of epitaxially grown graphene and Ru (0001) surfaces. *Appl Phys Lett* 2011; **99**: 163107.
104. Cui, Y, Gao, J and Jin, L *et al.* An exchange intercalation mechanism for the formation of a two-dimensional Si structure underneath graphene. *Nano Res* 2012; **5**: 352–60.
105. Jin, L, Fu, Q and Yang, Y *et al.* A comparative study of intercalation mechanism at graphene/Ru (0001) interface. *Surf Sci* 2013; **617**: 81–6.
106. Gierz, I, Suzuki, T and Weitz, RT *et al.* Electronic decoupling of an epitaxial graphene monolayer by gold intercalation. *Phys Rev B* 2010; **81**: 235408.
107. Wang, Z, Dong, A and Wei, M *et al.* Graphene as a surfactant for metal growth on solid surfaces: Fe on graphene/SiC (0001). *Appl Phys Lett* 2014; **104**: 181604.
108. Zhang, H, Fu, Q and Cui, Y *et al.* Growth mechanism of graphene on Ru (0001) and O_2 adsorption on the graphene/Ru (0001) surface. *J Phys Chem C* 2009; **113**: 8296–301.
109. Sutter, P, Sadowski, JT and Sutter, EA. Chemistry under cover: tuning metal—graphene interaction by reactive intercalation. *J Am Chem Soc* 2010; **132**: 8175–9.
110. Feng, X, Maier, S and Salmeron, M. Water splits epitaxial graphene and intercalates. *J Am Chem Soc* 2012; **134**: 5662–8.

111. Grånäs, E, Knudsen, J and Schröder, UA *et al.* Oxygen intercalation under graphene on Ir(111): energetics, kinetics, and the role of graphene edges. *ACS Nano* 2012; **6**: 9951–63.
112. Larciprete, R, Ulstrup, S and Lacovig, P *et al.* Oxygen switching of the epitaxial graphene–metal interaction. *ACS Nano* 2012; **6**: 9551–8.
113. Mu, R, Fu, Q and Jin, L *et al.* Visualizing chemical reactions confined under graphene. *Angew Chem Int Ed* 2012; **51**: 4856–9.
114. Jin, L, Fu, Q and Dong, A *et al.* Surface chemistry of CO on Ru (0001) under the confinement of graphene cover. *J Phys Chem C* 2014; **118**: 12391–8.
115. Yao, Y, Fu, Q and Zhang, Y *et al.* Graphene cover-promoted metal-catalyzed reactions. *Proc Natl Acad Sci USA* 2014; **111**: 17023–8.
116. Wu, G, More, KL and Johnston, CM *et al.* High-performance electrocatalysts for oxygen reduction derived from polyaniline, iron, and cobalt. *Science* 2011; **332**: 443–7.
117. Deng, DH, Yu, L and Chen, XQ *et al.* Iron encapsulated within pod-like carbon nanotubes for oxygen reduction reaction. *Angew Chem Int Ed* 2013; **52**: 371–5.
118. Deng, J, Yu, L and Deng, DH *et al.* Highly active reduction of oxygen on a FeCo alloy catalyst encapsulated in pod-like carbon nanotubes with fewer walls. *J Mater Chem A* 2013; **1**: 14868–73.
119. Chen, X, Xiao, J and Wang, J *et al.* Visualizing electronic interactions between iron and carbon by X-ray chemical imaging and spectroscopy. *Chem Sci* 2015; **6**: 3262–7.
120. Zheng, XJ, Deng, J and Wang, N *et al.* Podlike N-doped carbon nanotubes encapsulating FeNi alloy nanoparticles: high-performance counter electrode materials for dye-sensitized solar cells. *Angew Chem Int Ed* 2014; **53**: 7023–7.
121. Hu, Y, Jensen, JO and Zhang, W *et al.* Hollow spheres of iron carbide nanoparticles encased in graphitic layers as oxygen reduction catalysts. *Angew Chem Int Ed* 2014; **53**: 3675–9.
122. Zou, XC, Huang, XC and Goswami, A *et al.* Cobalt-embedded nitrogen-rich carbon nanotubes efficiently catalyze hydrogen evolution reaction at all pH values. *Angew Chem Int Ed* 2014; **53**: 4372–6.
123. Deng, J, Ren, P and Deng, D *et al.* Enhanced electron penetration through an ultrathin graphene layer for highly efficient catalysis of the hydrogen evolution reaction. *Angew Chem Int Ed* 2015; **54**: 2100–4.
124. Deng, J, Ren, PJ and Deng, DH *et al.* Highly active and durable non-precious-metal catalysts encapsulated in carbon nanotubes for hydrogen evolution reaction. *Energy Environ Sci* 2014; **7**: 1919–23.